Analytical and Numerical Methods in Shape Optimization

Helmut Harbrecht

no. 305

Diese Arbeit ist mit Unterstützung des von der Deutschen Forschungsgemeinschaft getragenen Sonderforschungsbereiches 611 an der Universität Bonn entstanden und als Manuskript vervielfältigt worden.

Bonn, November 2006

ANALYTICAL AND NUMERICAL METHODS IN SHAPE OPTIMIZATION

HELMUT HARBRECHT

Abstract. The present paper is intented to overview on analytical and numerical methods in shape optimization. We compute and analyse the shape Hessian in order to distinguish well-posed and ill-posed shape optimization problems. We introduce different discretization techniques of the shape and present existence and convergence results of approximate solutions in case of well-posedness. Finally, we survey on the efficient numerical solution of the state equation, including finite and boundary element methods as well as fictitious domain methods.

Introduction

Shape optimization is quite important for aircraft design, construction of bridges, electromagnetic shaping etc. Many problems that arise in application, particularly in structural mechanics, can be formulated as the minimization of functionals defined over a class of admissible domains. Such problems have been intensively studied in the literature in the past 25–30 years (see [33, 35, 42, 46], and the references therein). Especially, the development of efficient algorithms in shape optimization is of growing interest.

The present survey article is dedicated to analytical and numerical methods in shape optimization. We will view the shape optimization problem as an optimization problem in a Banach space by identifying the shape with its parametrization with respect to a fixed reference domain. Using a second order shape calculus we are able to compute the shape Hessian. Our ansatz ensures that the shape Hessian denotes in fact the second order Fréchet derivative of the given shape functional. Depending on the properties of the shape Hessian we can distinguish well-posed and ill-posed shape optimization problems. In case of well-posedness we are able to prove existence of approximate shapes and their convergence to the optimal domain.

We illustrate well-posedness and ill-posedness by two examples. Stationary free boundary problems, especially Bernoulli's free boundary problem (see e.g. [2, 25]) or electromagnetic shaping (see e.g. [6, 17, 41]), are generally well-posed problems. Whereas, we

Dedicated to Wolfgang L. Wendland on the occasion of his 70th birthday.

will show that compactly supported shape problems, such as L^2- or gradient tracking functionals, are ill-posed.

We present several numerical methods to solve the underlying state equation in an efficient way. Depending on the problem under consideration we propose to solve the state equation by boundary element methods, by the coupling of boundary and finite element methods, or by fictitious domain methods. We emphasize that all these methods have in common that they are *meshless*, that is, they do not need an explicit triangulation of the domain. Consequently, large domain deformations are realizable without remeshing. For sake of completeness, we also discuss the use of finite element methods.

The paper is organized as follows. The first section is dedicated to shape calculus. Computing first and second order shape derivatives, we are able to analyse the shape optimization problem at hand. Depending on the coercivity estimates of the shape Hessian we will distinguish between well-posed and ill-posed problems. Both cases are illustrated by an corresponding example. The second section is concerned with the discretization techniques of the shape. In particular, in case of well-posedness, we show that approximate shapes converge quasi-optimal with respect to the energy norm induced by the shape Hessian. Finally, the last section addresses the efficient numerical solution of the state equation.

In the following, in order to avoid the repeated use of generic but unspecified constants, by $C \lesssim D$ we mean that C can be bounded by a multiple of D, independently of parameters which C and D may depend on. Obviously, $C \gtrsim D$ is defined as $D \lesssim C$, and $C \sim D$ as $C \lesssim D$ and $C \gtrsim D$.

1. Analyzing shape optimization problems

1.1. **Shape calculus.** Let $\Omega \subset \mathbb{R}^n$ denote a sufficiently smooth simply connected domain with boundary $\Gamma := \partial\Omega$. Throughout this paper we shall focus on the following shape functional

$$J(\Omega) = \int_\Omega j\big(\mathbf{x}, u(\mathbf{x})\big) d\mathbf{x} \to \min, \tag{1.1}$$

where the state function u satisfies the boundary value problem

$$-\Delta u = f \text{ in } \Omega, \qquad u = g \text{ on } \Gamma. \tag{1.2}$$

Herein, we assume that $f, g : \mathbb{D} \to \mathbb{R}$ and $j : \mathbb{D} \times \mathbb{R} \to \mathbb{R}$ are sufficiently smooth functions, where $\mathbb{D} \subset \mathbb{R}^n$ denotes the hold all.

For a sufficiently smooth domain perturbation field $\mathbf{V} : \Omega \to \mathbb{R}^n$ we can define the perturbed domain $\Omega_\varepsilon[\mathbf{V}]$ as

$$\Omega_\varepsilon[\mathbf{V}] := \{(\mathbf{I} + \varepsilon\mathbf{V})(\mathbf{x}) : \mathbf{x} \in \Omega\}.$$

Then, the shape derivative of the functional (1.1) in the direction $\mathbf{V}$ is defined as the limes

$$\nabla J(\Omega)[\mathbf{V}] = \lim_{\varepsilon\to 0} \frac{J(\Omega_\varepsilon[\mathbf{V}]) - J(\Omega)}{\varepsilon}.$$

For $f \in C(\overline{\Omega})$ the directional shape derivative of the domain integral $\int_\Omega f(\mathbf{x})d\mathbf{x}$ is the boundary integral

$$\nabla\bigg(\int_\Omega f(\mathbf{x})d\mathbf{x}\bigg)[\mathbf{V}] = \int_\Gamma \langle \mathbf{V}, \mathbf{n}\rangle f(\mathbf{x})d\sigma_{\mathbf{x}},$$

where $\mathbf{n}$ denotes the outward unit normal to the boundary Γ. Thus, by the chain rule we obtain

$$\nabla J(\Omega)[\mathbf{V}] = \int_\Gamma \langle \mathbf{V}, \mathbf{n}\rangle j(\mathbf{x}, g)d\sigma_{\mathbf{x}} + \int_\Omega \frac{\partial j}{\partial u}(\mathbf{x}, u)du[\mathbf{V}]d\mathbf{x}.$$

Here, $du[\mathbf{V}]$ is the *local shape derivative*, defined pointwise by

$$du(\mathbf{x})[\mathbf{V}] = \lim_{\varepsilon\to 0} \frac{u_\varepsilon[\mathbf{V}](\mathbf{x}) - u(\mathbf{x})}{\varepsilon}, \quad \mathbf{x} \in \Omega \cap \Omega_\varepsilon.$$

It reads as

$$\Delta du[\mathbf{V}] = 0 \text{ in } \Omega, \qquad du[\mathbf{V}] = \langle \mathbf{V}, \mathbf{n}\rangle \frac{\partial(g-u)}{\partial \mathbf{n}} \text{ on } \Gamma, \tag{1.3}$$

cf. [14, 36, 43]. Introducing the adjoint state function p according to

$$-\Delta p = \frac{\partial j}{\partial u}(\cdot, u) \text{ in } \Omega, \qquad p = 0 \text{ on } \Gamma, \tag{1.4}$$

we can apply the Green's second formula to derive the boundary integral representation of the shape derivative

$$\nabla J(\Omega)[\mathbf{V}] = \int_\Gamma \langle \mathbf{V}, \mathbf{n}\rangle \left\{ j(\mathbf{x}, g) + \frac{\partial p}{\partial \mathbf{n}} \frac{\partial(g-u)}{\partial \mathbf{n}} \right\} d\sigma_{\mathbf{x}}. \tag{1.5}$$

We observe that the directional derivative lives completely on the free boundary, involving the Dirichlet-to-Neumann maps (often called the Steklov-Poincaré operator) of u and p. Consequently, as observed first by Hadamard [29], the shape gradient is a functional defined on the free boundary. In particular, it is obvious that it suffices to consider only boundary variations $\mathbf{V} : \Gamma \to \mathbb{R}^n$.

1.2. **Second order derivatives.** In order to discuss sufficient optimality conditions one has to take the shape Hessian into account. To this end, we introduce an n-dimensional reference manifold $\widehat{\Gamma}$ and consider a fixed boundary perturbation field, for example in direction of the outward normal $\widehat{\mathbf{n}}$. We suppose that the free boundary can be parameterized via a sufficiently smooth function r in terms of

$$\boldsymbol{\gamma} : \widehat{\Gamma} \to \Gamma, \quad \boldsymbol{\gamma}(\mathbf{x}) = \mathbf{x} + r(\mathbf{x})\widehat{\mathbf{n}}(\mathbf{x}). \tag{1.6}$$

That is, we can identify a domain with the scalar function r. Defining the standard variation

$$\boldsymbol{\gamma}_\varepsilon : \widehat{\Gamma} \to \Gamma_\varepsilon, \quad \boldsymbol{\gamma}_\varepsilon(\mathbf{x}) := \boldsymbol{\gamma}(\mathbf{x}) + \varepsilon dr(\mathbf{x})\widehat{\mathbf{n}}(\mathbf{x}), \tag{1.7}$$

where dr is again a sufficiently smooth scalar function, we obtain the perturbed domain $\Omega_\varepsilon[dr]$. Consequently, both, the shapes and their increments, can be seen as elements of a Banach space X. It turns out that we require $X = C^{2,\alpha}(\widehat{\Gamma})$ for some $\alpha > 0$ in the present case of pde-constraint shape functionals like (1.1), (1.2).

A quite canonical choice is to take the unit sphere

$$\mathbb{S} := \{\widehat{\mathbf{x}} \in \mathbb{R}^n : \|\widehat{\mathbf{x}}\| = 1\}$$

as reference manifold, which corresponds to the restriction to star-shaped domains. This choice will be considered in the sequel. Here and in the sequel, $\widehat{\mathbf{x}}$ will always indicate a point on the unit sphere. In particular, for a point $\mathbf{x} \in \mathbb{R}^n \setminus \{\mathbf{0}\}$ the notion $\widehat{\mathbf{x}}$ has to be understood as $\widehat{\mathbf{x}} := \mathbf{x}/\|\mathbf{x}\|$.

Observing that $\widehat{\mathbf{n}}(\widehat{\mathbf{x}}) = \widehat{\mathbf{x}}$ we can simplify the boundary parametrization (1.6) in accordance with

$$\boldsymbol{\gamma} : \mathbb{S} \to \Gamma, \quad \boldsymbol{\gamma}(\widehat{\mathbf{x}}) = r(\widehat{\mathbf{x}})\widehat{\mathbf{x}}. \tag{1.8}$$

Thus, observing the identities $\mathbf{V}(\mathbf{x}) = dr(\widehat{\mathbf{x}}) \cdot \widehat{\mathbf{x}}$ and

$$\langle \mathbf{V}, \mathbf{n} \rangle d\sigma_{\mathbf{x}} = dr(\widehat{\mathbf{x}}) \langle \widehat{\mathbf{x}}, \mathbf{n} \rangle d\sigma_{\mathbf{x}} = dr(\widehat{\mathbf{x}}) r(\widehat{\mathbf{x}})^{n-1} d\sigma_{\widehat{\mathbf{x}}},$$

one can rewrite the shape gradient (1.5) according to

$$\nabla J(r)[dr] = \int_{\mathbb{S}} dr r^{n-1} \left\{ j\big(\boldsymbol{\gamma}(\widehat{\mathbf{x}}), g\big) + \frac{\partial p}{\partial \mathbf{n}} \frac{\partial (g-u)}{\partial \mathbf{n}} \right\} d\sigma_{\widehat{\mathbf{x}}}. \tag{1.9}$$

Therefore, in accordance with [13, 14], the boundary integral representation of the shape Hessian is given by

$$\begin{aligned}\nabla^2 J(r)[dr_1, dr_2] = \int_{\mathbb{S}} & dr_1 dr_2 r^{n-2}(n-1)\left[j\big(\boldsymbol{\gamma}(\widehat{\mathbf{x}}), g\big) + \frac{\partial p}{\partial \mathbf{n}}\frac{\partial (g-u)}{\partial \mathbf{n}}\right] \\ & + dr_1 dr_2 r^{n-1}\frac{\partial}{\partial \widehat{\mathbf{x}}}\left[j\big(\boldsymbol{\gamma}(\widehat{\mathbf{x}}), g\big) + \frac{\partial p}{\partial \mathbf{n}}\frac{\partial (g-u)}{\partial \mathbf{n}}\right] \\ & + dr_1 r^{n-1}\left[\frac{\partial p}{\partial \mathbf{n}}\frac{\partial du[dr_2]}{\partial \mathbf{n}} - \frac{\partial dp[dr_2]}{\partial \mathbf{n}}\frac{\partial (g-u)}{\partial \mathbf{n}}\right] d\sigma_{\widehat{\mathbf{x}}}.\end{aligned} \tag{1.10}$$

Herein, the notion $\partial/\partial\widehat{\mathbf{x}}$ has to be understood in the sense of $\partial u/\partial\widehat{\mathbf{x}} = \langle \nabla u, \widehat{\mathbf{x}}\rangle$. Moreover, $du[dr_2]$ and $dp[dr_2]$ denote the local shape derivatives of the state function and the adjoint state function, which satisfy the boundary value problems (1.3) and

$$\begin{aligned} -\Delta dp[dr_2] &= du[dr_2]\cdot \frac{\partial^2 j}{\partial u^2}\big(\cdot, u\big) \quad \text{in } \Omega, \\ dp[dr_2] &= -dr_2\langle \widehat{\mathbf{x}}, \mathbf{n}\rangle \frac{\partial p}{\partial \mathbf{n}} \qquad \text{on } \Gamma, \end{aligned} \tag{1.11}$$

respectively.

The first two terms in the boundary integral representation (1.10) of the shape Hessian are associated with a bilinear form on $L^2(\mathbb{S})\times L^2(\mathbb{S})$. The last term involves a Dirichlet-to-Neumann map of dr_2 via (1.3) and (1.11). Consequently, as one readily verifies, the shape Hessian is a pseudo-differential operator of the order $+1$, see also [18, 19, 22].

1.3. **Necessary and sufficient optimality conditions.** Recall that, by introducing a reference manifold and a fixed variation field, we embedded the shape calculus into the Banach space $X = C^{2,\alpha}(\mathbb{S})$. We shall now consider the minimization of the shape functional (1.1), that is

$$J(r) \to \min, \qquad r \in X. \tag{1.12}$$

Herein, $J : X \mapsto \mathbb{R}$ defines a two times continuously differentiable functional, i.e., the gradient $\nabla J(r) \in X^\star$ as well as the Hessian $\nabla^2 J(r) \in \mathcal{L}(X, X^\star)$ exist for all $r \in X$, and the mappings $\nabla J(\cdot) : X \to X^\star$, $\nabla J^2(\cdot) : X \to \mathcal{L}(X, X^\star)$ are continuous.

Theorem 1 (Necessary first order optimality condition)**.** *Let $r^\star$ be a regular optimal solution for problem* (1.12)*. Then, there holds*

$$\nabla J(r^\star)[dr] = 0 \qquad \textit{for all } dr \in X. \tag{1.13}$$

Let $r^\star$ such that (1.13) hold, that is, $r^\star$ is a *stationary domain* of problem (1.12). According to [9], we find the following Taylor expansion for all domains $r \in X$, described by $r = r^\star + dr$, in the neighbourhood of $r^\star$

$$J(r) - J(r^\star) = 0 + \frac{1}{2}\nabla^2 J(r^\star)[dr, dr] + \eta(\|dr\|_X). \tag{1.14}$$

Herein, the second order Taylor remainder (cf. [9]) fulfills

$$|\eta(\|dr\|_X)| = o(\|dr\|_X)\|dr\|^2_{H^{1/2}(\mathbb{S})}. \tag{1.15}$$

The Taylor expansion (1.14) implies that $J(r^\star)$ is a strong regular local minimizer of second order if and only if $\nabla^2 J(r^\star)$ is *strictly* coercive. However, since the shape Hessian defines a pseudo-differential operator of the order $+1$, we cannot expect coercivity of the shape Hessian in the Banach space X. Coercivity can be expected only in the weaker space $H^{1/2}(\mathbb{S})$.

Theorem 2 ([22])**.** *The stationary domain $r^\star$ is a strong regular local minimizer of second order if and only if the shape Hessian is $H^{1/2}(\mathbb{S})$-coercive, that is*

$$\nabla^2 J(r^\star)[dr, dr] \gtrsim \|dr\|^2_{H^{1/2}(\mathbb{S})}. \tag{1.16}$$

We emphasize that the radial function $r^\star$ has to be in X to ensure (1.14) and (1.15), while a minimizer is stable if the shape Hessian is $H^{1/2}(\mathbb{S})$-coercive. For more details on this phenomenon, called *two-norm discrepancy*, we refer to [9, 10, 15, 22].

1.4. **Free boundary problems — a class of well-posed problems.** A bright class of generally well posed shape optimization problems issues from free boundary problems. Let $T \subset \mathbb{R}^n$ denote a bounded domain with boundary $\partial T = \Gamma$. Inside the domain T we assume the existence of a simply connected subdomain $S \subset T$ with boundary $\partial S = \Sigma$. The resulting annular domain $T \setminus \overline{S}$ is denoted by Ω. Figure 1 refers to the given topological setup.

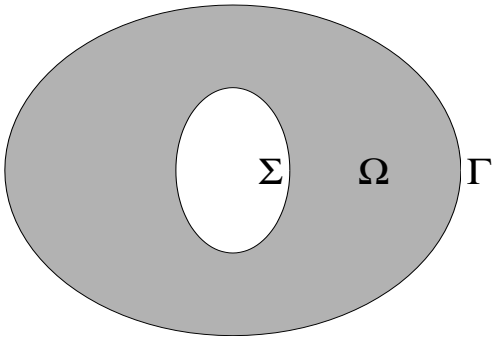

FIGURE 1. The domain Ω and its boundaries Γ and Σ.

We consider the following overdetermined boundary value problem in the annular domain Ω

$$\begin{aligned} -\Delta u &= f && \text{in } \Omega, \\ \|\nabla u\| = g, \quad u &= 0 && \text{on } \Gamma, \\ u &= h && \text{on } \Sigma, \end{aligned} \tag{1.17}$$

where $g, h > 0$ and $f \geq 0$ are sufficiently smooth functions. We like to stress that the positivity of the Dirichlet data imply that u is strictly positive in Ω. Hence, there holds the identity

$$\|\nabla u\| \equiv -\frac{\partial u}{\partial \mathbf{n}} \qquad \text{on } \Gamma$$

since u admits homogeneous Dirichlet data on Γ.

We arrive at a free boundary problem if the boundary Γ is the unknown. In other words, we seek a domain Ω with fixed boundary Σ and unknown boundary Γ such that the overdetermined boundary value problem (1.17) is solvable. For the existence of solutions of this generalized *exterior Bernoulli free boundary problem* we refer the reader to e.g. [2], see also [25] for the related *interior* free boundary problem. Results concerning the geometric form of the solutions can be found in [1] and the references therein.

Shape optimization provides an efficient tool to solve such free boundary value problems, cf. [11, 19, 34, 46]. We consider the cost functional

$$J(\Omega) = \int_\Omega \|\nabla u\|^2 - 2fu + g^2 d\mathbf{x} \tag{1.18}$$

with underlying state equation

$$\begin{aligned} -\Delta u &= f \qquad \text{in } \Omega, \\ u &= 0 \qquad \text{on } \Gamma, \\ u &= h \qquad \text{on } \Sigma. \end{aligned} \tag{1.19}$$

By virtue of the Gauss theorem we arrive at

$$J(\Omega) = \int_\Omega g^2 - fu d\mathbf{x} + \int_\Sigma \frac{\partial u}{\partial \mathbf{n}} h d\sigma_{\mathbf{x}}. \tag{1.20}$$

Since the boundary Σ is fixed, we conclude

$$\nabla\left(\int_\Sigma \frac{\partial u}{\partial \mathbf{n}} h d\sigma_{\mathbf{x}} \right)[\mathbf{V}] = \int_\Sigma \frac{\partial du[\mathbf{V}]}{\partial \mathbf{n}} h d\sigma_{\mathbf{x}}$$

for any sufficiently smooth variation field $\mathbf{V}$. Thus, one finds that the first and second shape derivatives are given as in Subsections 1.1 and 1.2, where the identity $p = -u$ holds. Consequently, the solution of the free boundary problem is equivalent to the shape optimization problem $J(\Omega) \to \min$ since the necessary condition of a minimizer of (1.18) reads as

$$\nabla J(\Omega)[\mathbf{V}] = \int_{\Gamma^\star} \langle \mathbf{V}, \mathbf{n} \rangle \left\{ g^2 - \left[\frac{\partial u}{\partial \mathbf{n}} \right]^2 \right\} d\sigma_{\mathbf{x}} \stackrel{!}{=} 0 \tag{1.21}$$

for all sufficiently smooth perturbation fields $\mathbf{V}$. Hence, via shape optimization a variational formulation of the condition

$$\frac{\partial u}{\partial \mathbf{n}} = -g \qquad \text{on } \Gamma$$

is induced. At least under certain circumstances we can prove the coercivity of the shape Hessian at a stationary domain in case of the present free boundary problem.

Theorem 3 ([19]). *Assume that $\Omega^\star$ is a stationary domain of the shape functional* (1.18). *Then, the shape Hessian is $H^{1/2}(\mathbb{S})$-coercive if*

$$\kappa + \left[\frac{\partial g}{\partial \mathbf{n}} - f\right] \Big/ g \geq 0 \qquad \text{on } \Gamma^\star,$$

where κ (resp. $2\mathcal{H}$ if $n = 3$) denotes the mean curvature. In particular, in the case $g \equiv const.$ and $f \equiv 0$, the shape Hessian is $H^{1/2}(\mathbb{S})$-coercive if the boundary $\Gamma^\star$ is convex (seen from inside).

The problem under consideration can be viewed as the prototype of a free boundary problem arising in many applications. For example, the growth of anodes in electrochemical processing might be modeled like above with $f \equiv 0$ and $g, h \equiv 1$.

In the two dimensional exterior magnetic shaping of liquid metals the state equation is an exterior Poisson equation and the uniqueness is ensured by a volume constraint of the domain Ω [6, 17, 41], see also the following subsection. However, since the shape functional involves the perimeter, which corresponds to the surface tension of the liquid, the energy space of the shape Hessian will be $H^1([0, 2\pi])$.

Remark 4. The detection of voids or inclusions in electrical impedance tomography is slightly different since the roles of Σ and Γ are interchanged [18, 44]. Particularly, this inverse problem is severely ill-posed, in contrary to the present class of problems. It has been proven in [18] that the shape Hessian is *not* strictly coercive in any $H^s(\mathbb{S})$ for all $s \in \mathbb{R}$.

1.5. **Compactly supported functionals — a class of ill-posed problems.** Engineers often aim in designing the shape of the domain $\Omega \in \mathbb{R}^n$ of definition for the underlying boundary value problem such that the state achieves prescribed values in a fixed subregion $B \subset\subset \Omega$, see also Figure 2. Mathematically speaking, this leads to an objective of the type

$$J(\Omega) = \int_B j\big(u(\mathbf{x}), \mathbf{x}\big) d\mathbf{x} \to \min, \tag{1.22}$$

where the state u satisfies the Poisson equation (1.2). In particular, for a given function u_d, the choice $j(u) = (u - u_d)^2$ yields the well known $L^2(B)$-tracking type functional. As the investigation of the stability of stationary domains will show, this class of shape optimization problems is severely ill-posed.

Extending the objective j by the trivial extension to the whole domain Ω the shape gradient and Hessian are given as in (1.5) and (1.10), respectively, where the adjoint

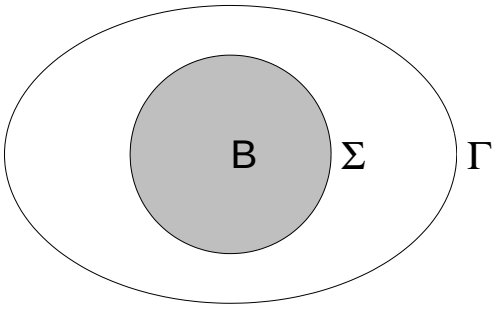

FIGURE 2. The domain Ω, the subdomain B, and the boundaries Γ and Σ.

state reads now as (cf. (1.4))

$$-\Delta p = \chi_B \cdot \frac{\partial j}{\partial u}\big(u(\cdot),\cdot\big) \text{ in } \Omega, \qquad p = 0 \text{ on } \Gamma, \tag{1.23}$$

and correspondingly the adjoint local shape derivative as (cf. (1.11))

$$\begin{aligned} -\Delta dp[dr_2] &= \chi_B \cdot du[dr_2]\frac{\partial^2 j}{\partial u^2}\big(u(\cdot),\cdot\big) \quad \text{in } \Omega, \\ dp[dr_2] &= -dr_2\langle \widehat{\mathbf{x}}, \mathbf{n}\rangle \frac{\partial p}{\partial \mathbf{n}} \qquad\qquad \text{on } \Gamma. \end{aligned} \tag{1.24}$$

Herein, χ_B denotes the characteristic function of B, i.e. $\chi_B = 1$ on B and $\chi_B = 0$ on $\mathbb{R}^n \setminus B$.

In the non-degenerated case we have $\partial(g-u)/\partial\mathbf{n} \not\equiv 0$ on Γ. Therefore, the necessary condition implies $\partial p/\partial \mathbf{n} \equiv 0$ on $\Gamma^\star$ since p is harmonic in $\Omega^\star \setminus \overline{B}$ admitting homogeneous Dirichlet data at $\Gamma^\star$ (cf. [20]). Consequently, the shape Hessian (1.10) simplifies at a stationary domain to

$$\nabla^2 J(\Omega^\star)[dr_1, dr_2] = \int_{\mathbb{S}} dr_1\, r^{n-1} \frac{\partial dp[dr_2]}{\partial \mathbf{n}} \cdot \frac{\partial (g-u)}{\partial \mathbf{n}}\, d\sigma_{\widehat{\mathbf{x}}}. \tag{1.25}$$

In particular, the adjoint local shape derivative $dp = dp[dr_2]$, defined in (1.24), admits homogeneous Dirichlet data. Employing the fundamental solution $E(\mathbf{x},\mathbf{y})$ of the Laplacian, given by

$$E(\mathbf{x},\mathbf{y}) := \begin{cases} -\dfrac{1}{2\pi}\log\|\mathbf{x}-\mathbf{y}\|, & \text{if } n = 2, \\ \dfrac{1}{4\pi}\dfrac{1}{\|\mathbf{x}-\mathbf{y}\|}, & \text{if } n = 3, \end{cases} \tag{1.26}$$

the adjoint local shape derivative $dp[dr_2]$ satisfies

$$dp[dr_2](\mathbf{x}) = \int_B E(\mathbf{x},\mathbf{y}) du[dr_2](\mathbf{y}) \frac{\partial^2 j}{\partial u^2}\big(\mathbf{y}, u(\mathbf{y})\big) d\sigma_{\mathbf{y}}, \qquad \mathbf{x} \in \Omega^\star.$$

Since the adjoint local shape derivative $dp[dr_2]$ and thus its Neumann data $\partial dp[dr_2]/\partial \mathbf{n}$ depend only on data living on B and $\operatorname{dist}(B, \Gamma^\star) > 0$ the shape Hessian (1.25) is compact.

Theorem 5 ([20]). *Assume that $\Omega^\star$ is a stationary solution of the shape functional* (1.22). *Then, the shape Hessian at $\Omega^\star$ defines a compact mapping $\nabla^2 J(\Omega^\star) : H^{1/2}(\Gamma) \to H^{-1/2}(\Gamma)$. It defines even an arbitrarily smoothing pseudo-differential operator if $\Omega^\star \in C^\infty$.*

Remark 6. Notice that, since tracking type functionals allow a reinterpretation as inverse problems (see e.g. [5]), the compactness of the shape Hessian at the minimizing domain refers directly to the ill-posedness of the underlying identification problem.

2. Shape approximation

2.1. **Nonlinear Ritz-Galerkin approximation.** In order to solve the minimization problem defined by (1.1) and (1.2), we are seeking the stationary points $r^\star \in X$ satisfying

$$\nabla J(r^\star)[dr] = 0 \quad \text{for all } dr \in X. \tag{2.1}$$

In accordance with [22] we shall introduce a Ritz-Galerkin method for the nonlinear equation (2.1). To this end, we restrict ourselves again to star-shaped domains and consider the gradient in terms of sphericals coordinates (1.9). Nevertheless, one can consider any fixed variation field with respect to a smooth reference manifold as well.

Let $\varphi_i : \mathbb{S} \to \mathbb{R}$ denote suitable ansatz functions and consider the ansatz space

$$V_N = \operatorname{span}\{\varphi_1, \varphi_2, \ldots, \varphi_N\} \subset X. \tag{2.2}$$

In practice, we will use the first N spherical harmonics in $\mathbb{R}^n$ as ansatz functions.

We now replace (2.1) by its finite dimensional counterpart:

$$\text{seek } r_N^\star \in V_N \text{ such that} \quad \nabla J(r_N^\star)[dr] = 0 \quad \text{for all } dr \in V_N. \tag{2.3}$$

Note that this is the necessary condition associated with the finite dimensional optimization problem

$$J(r_N) \to \min, \quad r_N \in V_N. \tag{2.4}$$

Concerning the existence and convergence of approximate shapes we have the following theorem.

Theorem 7 ([22]). *Assume that the shape Hessian is strictly $H^{1/2}(\mathbb{S})$-coercive at the stationary domain $r^\star \in X$. Then,* (2.4) *admits a unique solution $r_N^\star \in V_N$ provided*

that N is large enough. The approximation error stays in the energy norm proportional to the best approximation in V_N, that is

$$\|r_N^\star - r^\star\|_{H^{1/2}(\mathbb{S})} \lesssim \inf_{r_N \in V_N} \|r_N - r^\star\|_{H^{1/2}(\mathbb{S})}.$$

There exist different strategies to find $r_N \in V_N$ such that (2.3) holds. In general, one makes the ansatz $r_N = \sum_{i=1}^N r_i \varphi_i$ and considers the iterative scheme

$$\mathbf{r}^{(n+1)} = \mathbf{r}^{(n)} - h^{(n)} \mathbf{M}^{(n)} \mathbf{G}^{(n)}, \quad n = 0, 1, 2, \dots, \tag{2.5}$$

where $h^{(n)}$ is a suitable step width and

$$\mathbf{r}^{(n)} = \big(r_i^{(n)}\big)_{i=1,\dots,N}, \quad \mathbf{G}^{(n)} := \big(\nabla J(r_N^{(n)})[\varphi_i]\big)_{i=1,\dots,N}.$$

First order methods are the gradient method ($\mathbf{M}^{(n)} := \mathbf{I}$) or the quasi Newton method where $\mathbf{M}^{(n)}$ denotes a suitable approximation to the inverse shape Hessian. Choosing

$$\mathbf{M}^{(n)} := \big(\nabla^2 J(r_N^{(n)})[\varphi_i, \varphi_j]\big)^{-1}_{i,j=1,\dots,N}$$

we arrive at the Newton method, which converges much faster compared to the first order methods, see [16] for example. For a survey on available optimization algorithms we refer the reader to [12, 26].

The following statement is an immediate consequence of Theorem 7.

Corollary 8 ([19])**.** *Under the assumptions of Theorem 7 the iterants $r_N^{(n)}$ produced by algorithm* (2.5) *converge to $r_N^\star$ provided that the initial guess $r_N^{(0)}$ is properly chosen.*

2.2. **More flexible boundary representations.** If one intends to implement only first order shape optimization algorithms, one may employ a more general boundary representation than the restrictive approach (1.6), (1.7).

The boundary of a domain Ω can be represented by a bijective positive oriented function

$$\boldsymbol{\gamma} : \mathbb{S} \to \Gamma, \qquad \boldsymbol{\gamma}(\widehat{\mathbf{x}}) = \big[\gamma_1(\widehat{\mathbf{x}}), \dots, \gamma_n(\widehat{\mathbf{x}})\big]^T, \tag{2.6}$$

such that $\gamma_1, \dots, \gamma_n \in C^2(\mathbb{S})$. Consider again the ansatz space V_N from (2.2). To discretize the shape optimization problem we make this time the ansatz

$$\boldsymbol{\gamma}_N = \sum_{k=-N}^{N} \mathbf{a}_k \varphi_k \in V_N^n \tag{2.7}$$

with *vector-valued coefficients* $\mathbf{a}_k \in \mathbb{R}^n$.

On the one hand the ansatz (2.7) does not impose any restriction to the topology of the domain except for its gender. On the other hand the parametric representation (2.6) of the domain Ω is not unique. In fact, if $\Xi : \mathbb{S} \to \mathbb{S}$ denotes any smooth

bijective mapping, then the function $\boldsymbol{\gamma} \circ \Xi$ describes another parametrization of Ω. Consequently, one cannot expect convergence results like that of Theorem 7.

To avoid degenerated boundary representations one can apply from time to time a suitable remeshing algorithm. However, even for a large number of degrees of freedom, the surface, and thus the value of the cost functional, is changed considerably by remeshing. Consequently, it might happen that the shape optimization algorithm does not convergence. To our experience it is preferable to regularize the shape functional instead. It is quite obvious that, for numerical computations, a "nice" parametrization maps orthonormal tangents $\{\mathbf{t}_i\}_{i=1}^n$ on the parameter space $\mathbb{S}$ to orthogonal tangents on the boundary Γ, possibly with the same length on whole Γ. Therefore, consider the mesh functional

$$M(\Omega) = \int_{\mathbb{S}} \left\| \mathcal{T}(\widehat{\mathbf{x}}) - \frac{|\Gamma|^2}{|\mathbb{S}|^2} \mathbf{I} \right\|_F^2 d\sigma_{\widehat{\mathbf{x}}},$$

where $\mathcal{T}$ denotes the first fundamental tensor of differential geometry, given by

$$\mathcal{T}(\widehat{\mathbf{x}}) = \left[\left\langle \frac{\partial \boldsymbol{\gamma}(\widehat{\mathbf{x}})}{\partial \mathbf{t}_i}, \frac{\partial \boldsymbol{\gamma}(\widehat{\mathbf{x}})}{\partial \mathbf{t}_j} \right\rangle \right]_{i,j=1}^n,$$

and $\|\cdot\|_F$ denotes the Frobenius norm. Therefore, this mesh functional is identical to zero if and only if the first fundamental tensor of differential geometry is on the whole parameter space identical to $|\Gamma|^2/|\mathbb{S}|^2$-times the identity matrix, which is equivalent to the above claim. This motivates to solve for small $\beta > 0$ the *regularized* shape problem

$$J(\Omega) + \beta M(\Omega) \to \min_{\Omega \in \Upsilon}$$

instead of the original problem (1.1). It is well known that the best results are achieved when $\beta \to 0$ during the optimization procedure, see also [21].

2.3. **Computing domain integrals.** Boundary integrals can be computed by employing the parametric representation of the boundary. However, the evaluation of domain integrals

$$I(\Omega) := \int_\Omega f(\mathbf{x}) d\mathbf{x}, \tag{2.8}$$

where $f \in C(\overline{\Omega})$, requires a suitable triangulation of the domain. For two space dimensions such a triangulation can be constructed as follows.

We compute the points of intersection of the boundary curve Γ and the grid $\bigcup_{\mathbf{k} \in \mathbb{Z}^2} \partial Q_{j,\mathbf{k}}$, generated from the squares

$$Q_{j,\mathbf{k}} := [2^{-j} k_1, 2^{-j}(k_1+1)] \times [2^{-j} k_2, 2^{-j}(k_2+1)].$$

Then, we replace the boundary curve Γ by the piecewise linear curve $\widetilde{\Gamma}$ which connects these points by straight lines. The enclosed polygonal domain will be denoted by $\widetilde{\Omega}$.

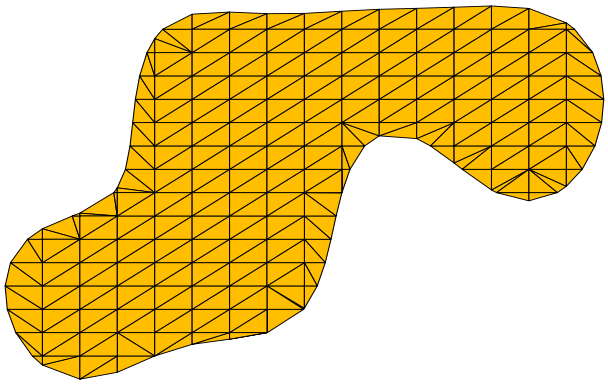

FIGURE 3. Triangulation of the domain.

We will next construct a suitable triangulation of $\widetilde{\Omega}$. We subdivide all elements $Q_{j,\mathbf{k}}$ that intersect the boundary $\widetilde{\Gamma}$ into suitable triangles to triangulate $Q_{j,\mathbf{k}} \cap \widetilde{\Omega}$. In the remaining part of $\widetilde{\Omega}$ we subdivide the elements $Q_{j,\mathbf{k}}$ into two triangles. Finally, we apply appropriate quadrature formulae on triangles. Figure 3 exemplifies a triangulation produced by our algorithm. Of course, the present algorithm produces also rather degenerated triangles. However, in connection with numerical quadrature, this does not matter.

In complete analogy one introduces in the three dimensional case a triangulation of the free surface and henceforth a tretrahedral mesh of the domain.

Theorem 9 ([21]). *Assume that $\Omega \in C^2$ and $f \in C^2(\mathbb{D})$. Then, the above quadrature algorithm computes the integral $I(\Omega)$ from (2.8) with accuracy $\mathcal{O}(h_j^2)$, where $h_j = 2^{-j}$, provided that the element quadrature formulae are exact for linear polynomials.*

3. Solving the state equation

3.1. **Boundary element methods.** In order to compute shape gradients and Hessians one only needs boundary values of the underlying state and adjoint state functions. However, the evaluation of the cost functional (1.1) seems to require the explicit knowledge of the state u on the complete domain Ω. At least in the case of free boundary problems this is not the case.

Thanks to a suitable Newton potential the functional (1.18) as well as its gradient and Hessian can be derived from the boundary data of a harmonic function. Thus, the use of boundary integral equations is highly attractive since their numerical solution requires only a triangulation of the boundary. That way, large domain deformations become realizable without remeshing as necessary for example when using finite element methods. Additionally, compared to finite element methods, the complexity is

even reduced if we apply modern boundary element methods like e.g. the *multipole method* [24], $\mathcal{H}$*-matrices* [28], or the *wavelet Galerkin scheme* [8].

We shall now introduce the Newton potential N_f that satisfies

$$-\Delta N_f = f \qquad \text{in } \Omega. \tag{3.1}$$

This Newton potential is supposed to be explicitly known or computed once with sufficiently high accuracy. Since the computational domain $\widehat{\Omega}$ can be chosen fairly simple, efficient solution techniques can be used without further difficulties.

Via the ansatz

$$u = N_f + v \tag{3.2}$$

the state equation (1.19) is transformed to the following Dirichlet problem for the Laplacian

$$\begin{aligned} \Delta v &= 0 && \text{in } \Omega, \\ v &= -N_f && \text{on } \Gamma, \\ v &= h - N_f && \text{on } \Sigma. \end{aligned} \tag{3.3}$$

To reformulate the cost functional (1.18) we apply integration by parts (cf. (1.20))

$$J(\Omega) = \int_\Omega \|\nabla u\|^2 - 2fu + g^2 d\mathbf{x} = \int_\Omega g^2 - (N_f + v) f d\mathbf{x} + \int_\Sigma \frac{\partial (N_f + v)}{\partial \mathbf{n}} h d\sigma_{\mathbf{x}}. \tag{3.4}$$

Green's second formula implies the identity

$$\int_\Omega v f d\mathbf{x} = \int_{\partial\Omega} \frac{\partial v}{\partial \mathbf{n}} N_f \, d\sigma_{\mathbf{x}} - \int_{\partial\Omega} v \frac{\partial N_f}{\partial \mathbf{n}} \, d\sigma_{\mathbf{x}} = \int_{\partial\Omega} N_f \frac{\partial u}{\partial \mathbf{n}} \, d\sigma_{\mathbf{x}} - \int_\Sigma h \frac{\partial N_f}{\partial \mathbf{n}} \, d\sigma_{\mathbf{x}}.$$

Inserting this equation into (3.4) gives

$$J(\Omega) = \int_\Omega g^2 - N_f f d\mathbf{x} + \int_\Sigma \frac{\partial (2N_f + v)}{\partial \mathbf{n}} h \, d\sigma_{\mathbf{x}} - \int_{\partial\Omega} N_f \frac{\partial u}{\partial \mathbf{n}} \, d\sigma_{\mathbf{x}}. \tag{3.5}$$

Consequently, both, the cost functional and its gradient (cf. (1.21)) can be computed provided that the normal derivative $\partial u / \partial \mathbf{n}$ is known. Its knowledge is therefore sufficient to perform a first order optimization method. Recall that the remaining domain integral in (3.5) can be computed according to Subsection 2.3.

The ansatz (3.2) leads to the normal derivative $\partial u / \partial \mathbf{n}$ according to

$$\frac{\partial u}{\partial \mathbf{n}} = \frac{\partial v}{\partial \mathbf{n}} + \frac{\partial N_f}{\partial \mathbf{n}}$$

with the Newton potential N_f defined via (3.1) and v satisfying the boundary value problem (3.3). We introduce the *single layer operator* $\mathcal{V}$ and the *double layer operator*

$\mathcal{K}$ defined by

$$\begin{aligned}(\mathcal{V}u)(\mathbf{x}) &:= \int_{\partial\Omega} E(\mathbf{x},\mathbf{y})u(\mathbf{y})d\sigma_{\mathbf{y}},\\ (\mathcal{K}u)(\mathbf{x}) &:= \int_{\partial\Omega} \frac{\partial E(\mathbf{x},\mathbf{y})}{\partial \mathbf{n}(\mathbf{y})}u(\mathbf{y})d\sigma_{\mathbf{y}},\end{aligned} \qquad \mathbf{x}\in\partial\Omega,$$

where the fundamental solution $E(\mathbf{x},\mathbf{y})$ is given by (1.26). Thus, the normal derivative of v is derived by the following boundary integral equation, the so-called *Dirichlet-to-Neumann map*,

$$\mathcal{V}\frac{\partial v}{\partial \mathbf{n}} = \Big(\frac{1}{2}+\mathcal{K}\Big)(h\chi_\Sigma - N_f). \tag{3.6}$$

Remark 10. Via boundary element methods also second order derivatives of the state function, as required for the shape Hessian, become computable and thus a Newton method can be realized. For sake of brevity we skip the details and refer the reader to [16, 19] for the details.

3.2. **Coupling of FEM and BEM.** In difference to the previous subsection the adjoint state depends directly on the state if we consider compactly supported shape functionals. Fortunately, the coupling of finite element methods (FEM) and boundary element methods (BEM) will essentially retain all the structural and computational advantages of treating the free boundary by boundary integral equations.

Let $\Omega\in\mathbb{R}^n$, $n=2,3$, be a simply connected domain with boundary $\Gamma := \partial\Omega$ and assume a fixed subdomain $B\subset\Omega$, see also Figure 2. Consider the shape optimization problem (1.22), where the state u satisfies the Poisson equation (1.2). The adjoint state function p, involved in the shape gradient (1.5), satisfies the boundary value problem (1.23). Thus, the adjoint state depends on the actual state u. Consequently, a numerical method for solving the state equation (1.2) should provide a fast access to u in the set B, like finite element methods. However, we like to preserve the advantages of boundary element methods to treat the free boundary Γ. This suggests to couple finite element methods and boundary element methods in order to compute the state and its adjoint.

We consider again the Newton potential (3.1) to resolve the inhomogeneity of the state equation (1.2) by the ansatz (3.2). Consequently, in view of the adjoint state equation (1.23), it suffices to consider a numerical method to solve

$$\begin{aligned} -\Delta v &= f && \text{in } B,\\ \Delta v &= 0 && \text{in } \Omega\setminus\overline{B},\\ v &= g && \text{on } \Gamma.\end{aligned} \tag{3.7}$$

We set $\Sigma := \partial B$ and assume the normal vectors $\mathbf{n}$ at Γ and Σ to point into $\Omega\setminus\overline{B}$, cf. Figure 2 for the topological situation. Then, (3.7) can be split in the following two

coupled boundary value problems

$$
\begin{aligned}
&-\Delta v = f \text{ in } B, \qquad \Delta v = 0 \text{ on } \Omega \setminus \overline{B}, \qquad v = g \text{ on } \Gamma, \\
&\lim_{\substack{\mathbf{y}\to\mathbf{x}\\ \mathbf{y}\in B}} v(\mathbf{y}) = \lim_{\substack{\mathbf{y}\to\mathbf{x}\\ \mathbf{y}\in\Omega\setminus\overline{B}}} v(\mathbf{y}), \quad \lim_{\substack{\mathbf{y}\to\mathbf{x}\\ \mathbf{y}\in B}} \frac{\partial v}{\partial \mathbf{n}}(\mathbf{y}) = \lim_{\substack{\mathbf{y}\to\mathbf{x}\\ \mathbf{y}\in\Omega\setminus\overline{B}}} \frac{\partial v}{\partial \mathbf{n}}(\mathbf{y}) \quad \text{for all } \mathbf{x}\in\Sigma.
\end{aligned} \tag{3.8}
$$

We introduce the *single layer operator* $\mathcal{V}_{\Phi\Psi}$, the *double layer operator* $\mathcal{K}_{\Phi\Psi}$, the *adjoint double layer operator* $\mathcal{K}^\star_{\Psi\Phi}$ and the *hypersingular operator* $\mathcal{W}_{\Phi\Psi}$ with respect to the boundaries $\Phi, \Psi \in \{\Gamma, \Sigma\}$ by

$$
\begin{aligned}
(\mathcal{V}_{\Phi\Psi}u)(\mathbf{x}) &:= \int_\Phi E(\mathbf{x},\mathbf{y})u(\mathbf{y})d\sigma_{\mathbf{y}}, \\
(\mathcal{K}_{\Phi\Psi}u)(\mathbf{x}) &:= \int_\Phi \frac{\partial E(\mathbf{x},\mathbf{y})}{\partial \mathbf{n}(\mathbf{y})}u(\mathbf{y})d\sigma_{\mathbf{y}}, \\
(\mathcal{K}^\star_{\Phi\Psi}u)(\mathbf{x}) &:= \int_\Phi \frac{\partial}{\partial \mathbf{n}(\mathbf{x})}E(\mathbf{x},\mathbf{y})u(\mathbf{y})d\sigma_{\mathbf{y}}, \\
(\mathcal{W}_{\Phi\Psi}u)(\mathbf{x}) &:= -\frac{\partial}{\partial \mathbf{n}(\mathbf{x})}\int_\Phi \frac{\partial E(\mathbf{x},\mathbf{y})}{\partial \mathbf{n}(\mathbf{y})}u(\mathbf{y})d\sigma_{\mathbf{y}},
\end{aligned}
\qquad \mathbf{x}\in\Psi,
$$

where the fundamental solution $E(\mathbf{x},\mathbf{y})$ is defined as in (1.26).

Finally, introducing the variables $\sigma_\Sigma := (\partial v/\partial \mathbf{n})|_\Sigma$ and $\sigma_\Gamma := (\partial v/\partial \mathbf{n})|_\Gamma$, the coupled system (3.8) yields the following nonlocal boundary value problem:

Find $(v, \sigma_\Sigma, \sigma_\Gamma) \in H^1(B) \times H^{-1/2}(\Sigma) \times H^{-1/2}(\Gamma)$ such that

$$
\begin{aligned}
&-\Delta v = f \text{ in } B, \qquad \Delta v = 0 \text{ on } \Omega \setminus \overline{B}, \\
&-\mathcal{W}_{\Sigma\Sigma}v - \mathcal{W}_{\Gamma\Sigma}g + \Big(\frac{1}{2} - \mathcal{K}^\star_{\Sigma\Sigma}\Big)\sigma_\Sigma - \mathcal{K}^\star_{\Gamma\Sigma}\sigma_\Gamma = \sigma_\Sigma \quad \text{on } \Sigma, \\
&\Big(\frac{1}{2} - \mathcal{K}_{\Sigma\Sigma}\Big)v - \mathcal{K}_{\Gamma\Sigma}g + \mathcal{V}_{\Sigma\Sigma}\sigma_\Sigma + \mathcal{V}_{\Gamma\Sigma}\sigma_\Gamma = 0 \quad \text{on } \Sigma, \\
&-\mathcal{K}_{\Sigma\Gamma}v + \Big(\frac{1}{2} - \mathcal{K}_{\Gamma\Gamma}\Big)g + \mathcal{V}_{\Sigma\Gamma}\sigma_\Sigma + \mathcal{V}_{\Gamma\Gamma}\sigma_\Gamma = 0 \quad \text{on } \Gamma.
\end{aligned} \tag{3.9}
$$

This system is the so-called *two integral formulation*, which is equivalent to our original model problem (3.7), see for example [7, 30].

The nonlocal boundary value problem (3.9) can be solved e.g. along the lines of [31, 32]. Finite elements are applied to discretize the Poisson equation on B. The system matrices arising from the boundary integral operators are discretized by suitable wavelet bases. That way, applying wavelet matrix compression, the complexity is reduced (cf. [31]) and optimal preconditioners are available (cf. [32]). We refer the reader to [20] for the details concerning our actual realization.

3.3. **Fictitious domain methods.** The above mentioned techniques are not applicable to general shape functionals or to state equations involving elliptic differential operators with non-constant coefficients. Fictitious domain methods (FDM) offer a

convenient tool to deal with such shape optimization problems while the complicated remeshing, required for finite element methods, is still avoided. We refer the reader to e.g. [33, 37, 40, 45] for FDM in shape optimization.

To solve a boundary value problem with FDM, one embeds the *intrinsic domain* into a larger, but much simpler, *fictitious domain* $\mathbb{T}$, for example, a periodic n-cube. The next step is to construct from the original problem some auxiliary problem on the fictitious domain such that the solutions of this auxiliary and the original problem coincide on the intrinsic domain.

However, the success of FDM was limited since traditional methods suffer from low orders of convergence. For instance, the FD-Lagrange multiplier approach converges only as $\mathcal{O}(h^{1/2})$ in the energy norm when approximating from uniform grids with mesh size h (see [23]). Even adaptive schemes cannot overcome this restriction: the rate of convergence of standard (i.e. based on isotropic refinements) adaptive methods is limited by $\mathcal{O}(N^{-1/2})$ and $\mathcal{O}(N^{-1/4})$ in two and three spatial dimensions, respectively, when spending N degrees of freedom, independently of the order of the approximation spaces (see [39] for a more detailed discussion).

These difficulties arise from non-smooth extensions of the solution to the outside of the intrinsic domain. In particular, the approximation near the boundary is rather poor. Unfortunately, exactly the boundary data are the relevant data which enter the shape derivatives.

In [38, 39] a rather novel and promising *smoothness preserving* fictitious domain method (SPFD) has been proposed which realizes higher orders of convergence due to smooth extensions of the solution. The capability of this method in the context of shape optimization problems has been demonstrated [21].

Consider the state equation (1.2), possibly with the more general elliptic differential operator $A : H^2(\mathbb{T}) \to L^2(\mathbb{T})$ instead of $-\Delta$, and assume the right hand side f to be in $L^2(\mathbb{T})$. Then, since the boundary Γ is C^2, the solution of the state equation will be in $H^2(\Omega)$. The crucial idea of the SPFD-method is to start with the following least-squares functional on $H^2(\mathbb{T})$: find $u^+ \in H^2(\mathbb{T})$ such that

$$\Phi(u^+) = \|P(Au^+ - f)\|^2_{L^2(\mathbb{T})} + \|u^+|_\Gamma - g\|^2_{H^{3/2}(\Gamma)} \to \min, \tag{3.10}$$

where $P : L^2(\mathbb{T}) \to L^2(\mathbb{T})$ is such that Pv is the extension by zero of the restriction to Ω of $v \in L^2(\mathbb{T})$. Applying a suitable discretization, the approximate solution to (3.10) seems to be in fact smooth, as the numerical results in [21, 39] indicate. However, a strict proof is only available under additional assumptions, see [38, 39] for the details.

3.4. **Finite element methods.** Finite element discretizations require a suitable triangulation of the *varying* domain. To apply efficient solution techniques like multigrid

methods one needs a sequence of nested trial spaces. Such sequences can easily be defined if the given triangulation is nested.

On curved domains one can construct nested meshes via parametrization. We shall assume that the domain Ω is given as a collection of smooth patches. More precisely, let $\square := [0,1]^n$ denote the unit n-cube. The domain $\Omega \in \mathbb{R}^n$ is partitioned into a finite number of *patches*

$$\Omega = \bigcup_{i=1}^{M} \Omega_i, \qquad \Omega_i = \boldsymbol{\kappa}_i(\square), \qquad i = 1, 2, \ldots, M,$$

where each $\boldsymbol{\kappa}_i : \square \to \Omega_i$ defines a diffeomorphism of $\square$ onto Ω_i. The intersection $\Omega_i \cap \Omega_j$, $i \neq j$, of the patches Ω_i and Ω_j is supposed to be either $\emptyset$ or a lower dimensional face.

A mesh of level j on Ω is induced by dyadic subdivisions of depth j of the unit cube into 2^{nj} cubes. This generates $2^{nj}M$ *elements* (or elementary domains). In order to ensure that the collection of elements on the level j forms a regular mesh on Ω, the parametric representation is subjected to the following *matching condition*: For all $\mathbf{y} \in \Omega_i \cap \Omega_j$ exists a bijective, affine mapping $\Xi : \square \to \square$ such that $\boldsymbol{\kappa}_i(\mathbf{x}) = (\boldsymbol{\kappa}_j \circ \Xi)(\mathbf{x}) = \mathbf{y}$ for $\mathbf{x} \in \square$ with $\boldsymbol{\kappa}_i(\mathbf{x}) = \mathbf{y}$. We refer to Figure 5 for corresponding meshes on level $j = 4$ consisting of $M = 5$ patches.

For shape optimization we need meshes for the varying domain Ω. At least for small domain variations one can map a nested triangulation of a reference domain $\widehat{\Omega}$ via a piecewise smooth diffeomorphism to the actual domain Ω. For example, having a parametrization $\{\widehat{\boldsymbol{\kappa}}_i\}$ of $\widehat{\Omega}$ in the above spirit at hand one can in case of the ansatz (1.6), (1.7) construct smooth mappings $\Theta_i = \Theta_i(r)$ such that $\Omega = \Omega(r)$ has the representation

$$\Omega = \bigcup_{i=1}^{M} \Omega_i, \qquad \Omega_i = \boldsymbol{\kappa}_i(\square) = (\Theta_i \circ \widehat{\boldsymbol{\kappa}}_i)(\square), \qquad i = 1, 2, \ldots, M,$$

where the matching condition still holds. That way, we will obtain a hierarchy on meshes on the domain Ω.

For illustrational reasons we shall consider two spatial dimensions and star-shaped domains, i.e., the unit circle as reference domain $\widehat{\Omega}$. In this case we are even able to construct directly the parametrization $\{\boldsymbol{\kappa}_i\}$ of the domain Ω. To that end, we assume the parametrization $\boldsymbol{\gamma}$ (2.6) to be defined as 2π-periodic function on the interval $[0, 2\pi]$. Then, for arbitrary values $0 \leq s < t \leq 2\pi$, the map

$$\boldsymbol{\kappa}_{i,1}(x, y) = \frac{1+y}{2} \cdot \boldsymbol{\gamma}\big(xs + (1-x)t\big), \quad (x, y) \in \square,$$

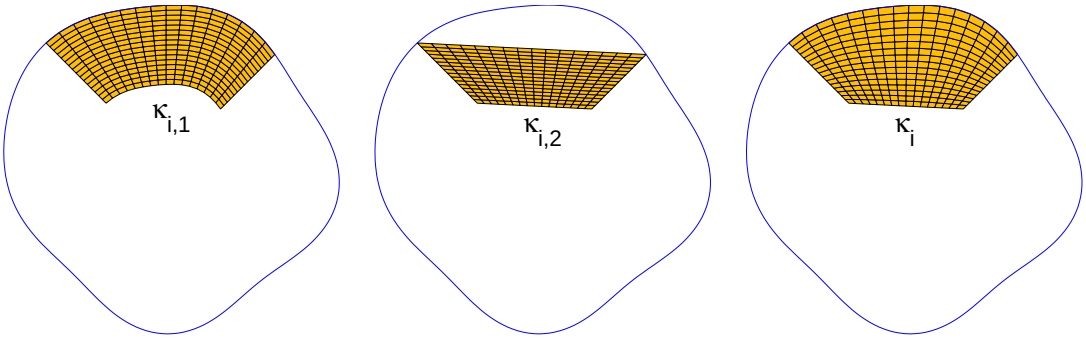

FIGURE 4. The images of the diffeomorphisms $\boldsymbol{\kappa}_{i,1}$ and $\boldsymbol{\kappa}_{i,2}$ and the final patch.

defines a curved patch where one edge coincides with the piece $\boldsymbol{\gamma}([s,t])$ of the boundary curve Γ, see the left plot of Figure 4. A quadriliteral patch that connects the four endpoints of the latter curved one is given by

$$\boldsymbol{\kappa}_{i,2}(x,y) = \frac{(1+y)}{2}\big\{(1-x)\boldsymbol{\gamma}(t) + x\boldsymbol{\gamma}(s)\big\}, \quad (x,y) \in \square,$$

Combining both mappings according to

$$\boldsymbol{\gamma}_i(x,y) = y \cdot \boldsymbol{\kappa}_{i,1}(x,y) + (1-y) \cdot \boldsymbol{\kappa}_{i,2}(x,y), \quad (x,y) \in \square,$$

leads to the final curved patch whose first edge coincides with Γ while the other edges are straight lines. That way, one can easily construct the parametric representation of the domain. A visualization of the final mesh on level $j = 4$ of the unit circle and the domain Ω is found in Figure 5. The present construction can be extended to general reference domains and to higher dimensions. Similar constructions are realizable in case of simplicial meshes.

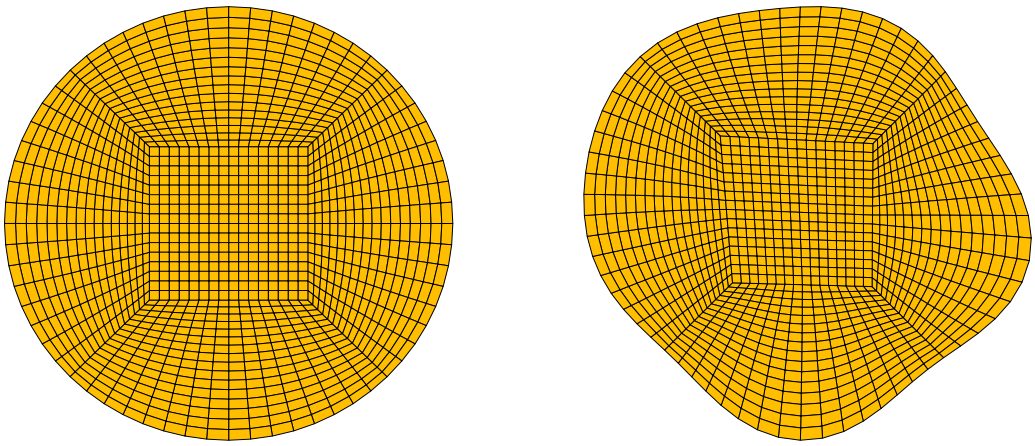

FIGURE 5. The quadriliteral mesh of the reference domain $\mathbb{S}$ and the domain Ω.

Finally, we can define the ansatz functions via parametrization, lifting for example Lagrangian finite elements from $\square$ by using the mappings $\boldsymbol{\kappa}_i$ and gluing across patch boundaries. This yields the promised sequence of nested trial spaces. Thus, the efficient numerical solution of boundary value problems on Ω by multigrid schemes will be straightforward, see e.g. [3, 4, 27].

References

[1] A. Acker. On the geometric form of Bernoulli configurations. *Math. Meth. Appl. Sci.* 10:1–14, 1988.

[2] H.W. Alt and L.A. Caffarelli. Existence and regularity for a minimum problem with free boundary. *J. reine angew. Math.*, 325:105–144, 1981.

[3] D. Braess. *Finite elements. Theory, fast solvers, and applications in solid mechanics*. Second edition. Cambridge University Press, Cambridge, 2001.

[4] J.H. Bramble. *Multigrid methods*. Pitman Research Notes in Mathematics Series, 294. Longman Scientific & Technical, Harlow, 1993.

[5] D. Chenais and E. Zuazua. Controllability of an elliptic equation and its finite difference approximation by the shape of the domain. *Numer. Math.* 95:63-99, 2003.

[6] O. Colaud and A. Henrot. Numerical approximation of a free boundary problem arising in electromagnetic shaping. *SIAM J. Numer. Anal.*, 31:1109–1127, 1994.

[7] M. Costabel and E.P. Stephan. Coupling of finite element and boundary element methods for an elasto-plastic interface problem. *SIAM J. Numer. Anal.*, 27:1212–1226, 1988.

[8] W. Dahmen, H. Harbrecht and R. Schneider. Compression techniques for boundary integral equations — optimal complexity estimates. *SIAM J. Numer. Anal.*, 43:2251–2271, 2006.

[9] M. Dambrine. On variations of the shape Hessian and sufficient conditions for the stability of critical shapes. *RACSAM, Rev. R. Acad. Cien. Serie A. Mat.* 96:95–121, 2002.

[10] M. Dambrine and M. Pierre. About stability of equilibrium shapes. *M2AN Math. Model. Numer. Anal.* 34:811-834, 2000.

[11] M. Delfour and J.-P. Zolesio. *Shapes and Geometries*. SIAM, Philadelphia, 2001.

[12] J.E. Dennis and R.B. Schnabel. *Numerical Methods for Nonlinear Equations and Unconstrained Optimization Techniques*. Prentice-Hall, Englewood Cliffs, 1983.

[13] K. Eppler. Boundary integral representations of second derivatives in shape optimization. *Discussiones Mathematicae (Differential Inclusion Control and Optimization)*, 20:63–78, 2000.

[14] K. Eppler. Optimal shape design for elliptic equations via BIE-methods. *J. of Applied Mathematics and Computer Science*, 10:487–516, 2000.

[15] K. Eppler. Second derivatives and sufficient optimality conditions for shape functionals. *Control & Cybernetics*. 29:485–512, 2000.

[16] K. Eppler and H. Harbrecht. Second Order Shape Optimization using Wavelet BEM. *Optim. Methods Softw.*, 21:135–153, 2006.

[17] K. Eppler and H. Harbrecht. Exterior Electromagnetic Shaping using Wavelet BEM. *Math. Meth. Appl. Sci.*, 28:387–405, 2005.

[18] K. Eppler and H. Harbrecht. A regularized Newton method in electrical impedance tomography using shape Hessian information. *Control & Cybernetics*, 34:203–225, 2005.

[19] K. Eppler and H. Harbrecht. Efficient treatment of stationary free boundary problems. *Appl. Numer. Math.*, 56:1326–1339, 2006.

[20] K. Eppler and H. Harbrecht. Coupling of FEM and BEM in Shape Optimization. *Numer. Math.*, 104:47–68, 2006.

[21] K. Eppler, H. Harbrecht, and M.S. Mommer. A new fictitious domain method in shape optimization. *WIAS-Preprint 1117*, WIAS Berlin, 2006. submitted to Comput. Optim. Appl.

[22] K. Eppler, H. Harbrecht, and R. Schneider. On convergence in elliptic shape optimization. *WIAS-Preprint 1016*, WIAS Berlin, 2005. to appear in *SIAM J. Control Optim.*

[23] R. Glowinski, T.W. Pan, and J. Periaux. A fictitious domain method for Dirichlet problem and applications. *Comput. Methods Appl. Mech. Eng.*, 111:283–303, 1994.

[24] L. Greengard and V. Rokhlin. A fast algorithm for particle simulation. *J. Comput. Phys.*, 73:325–348, 1987.

[25] M. Flucher and M. Rumpf. Bernoulli's free-boundary problem, qualitative theory and numerical approximation. *J. reine angew. Math.*, 486:165–204, 1997.

[26] Ch. Grossmann and J. Terno. *Numerik der Optimierung*. Teubner, Stuttgart, 1993.

[27] W. Hackbusch. *Multigrid methods and applications*. Springer Series in Computational Mathematics, 4. Springer-Verlag, Berlin, 1985.

[28] W. Hackbusch and B.N. Khoromskij. A sparse $\mathcal{H}$-matrix arithmetic. II: Application to multi-dimensional problems. *Computing*, 64:21–47, 2000.

[29] J. Hadamard. *Lessons on Calculus of Variations*. Gauthier–Villiars, Paris, 1910.

[30] H. Han. A new class of variational formulation for the coupling of finite and boundary element methos. *Journal of Computational Mathematics*, 8(3):223–232, 1990.

[31] H. Harbrecht, F. Paiva, C. Pérez, and R. Schneider. Biorthogonal wavelet approximation for the coupling of FEM-BEM. *Numer. Math.*, 92:325–356, 2002.

[32] H. Harbrecht, F. Paiva, C. Pérez, and R. Schneider. Wavelet preconditioning for the coupling of FEM-BEM. *Numer. Linear Algebra Appl.*, 3:197–222, 2003.

[33] J. Haslinger and P. Neitaanmäki. *Finite element approximation for optimal shape, material and topology design, 2nd edition*. Wiley, Chichester, 1996.

[34] J. Haslinger, T. Kozubek, K. Kunisch and G. Peichl. Shape optimization and fictitious domain approach for solving free boundary value problems of Bernoulli type. *Computational Optimization and Applications*, 26:231–251, 2003.

[35] A.M. Khludnev and J. Sokołowski. *Modelling and control in solid mechanics*. Birkhäuser, Basel, 1997.

[36] A. Kirsch. The domain derivative and two applications in inverse scattering theory. *Inverse Problems*, 9:81–96, 1993.

[37] K. Kunisch and G. Peichl. Shape optimization for mixed boundary value problems on an embedding domain method. *Dyn. Contin. Discrete Impulsive Syst.*, 4:439–478, 1998.

[38] M.S. Mommer. A Smoothness Preserving Fictitious Domain Method for Elliptic Boundary Value Problems. *IMA J. Numer. Anal.*, 26:503–524, 2006.

[39] M.S. Mommer. Towards a Fictitious Domain Method with Optimally Smooth Solutions. PhD thesis, RWTH-Aachen, published online by the RWTH-Aachen (2005).

[40] P. Neitaanmäki und D. Tiba. An embedding of domain approach in free boundary problems and optimal design. *SIAM J. Control Optim.*, 33:1587–1602, 1995.

[41] M. Pierre and J.-R. Roche. Computation of free surfaces in the electromagnetic shaping of liquid metals by optimization algorithms. *Eur. J. Mech, B/Fluids*, 10: 489–500, 1991.

[42] O. Pironneau. *Optimal shape design for elliptic systems*. Springer, New York, 1983.

[43] R. Potthast. Fréchet-Differenzierbarkeit von Randintegraloperatoren und Randwertproblemen zur Helmholtzgleichung und den zeitharmonischen Maxwellgleichungen. PhD Thesis, Uni Göttingen, 1994.

[44] J.-R. Roche and J. Sokolowski. Numerical methods for shape identification problems. *Control Cybern.*, 25:867–894, 1996.

[45] T. Slawig. A formula for the derivative with respect to domain variations in Navier–Stokes flow based on an embedding domain method. *SIAM J. Control Optim.*, 42:495–512, 2003.

[46] J. Sokolowski and J.-P. Zolesio. *Introduction to Shape Optimization*. Springer, Berlin, 1992.

Helmut Harbrecht, Institut für Angewandte Mathematik, Universität Bonn, Wegelerstr. 6, 53115 Bonn, Germany.

E-mail address: harbrecht@iam.uni-bonn.de

Bestellungen nimmt entgegen:

Institut für Angewandte Mathematik
der Universität Bonn
Sonderforschungsbereich 611
Wegelerstr. 6
D - 53115 Bonn

Telefon: 0228/73 4882
Telefax: 0228/73 7864
E-mail: link@wiener.iam.uni-bonn.de http://www.iam.uni-bonn.de/sfb611/

Verzeichnis der erschienenen Preprints ab No. 275

275. Otto, Felix; Reznikoff, Maria G.: Slow Motion of Gradient Flows

276. Albeverio, Sergio; Baranovskyi, Oleksandr; Pratsiovytyi, Mykola; Torbin, Grygoriy: The Ostrogradsky Series and Related Probability Measures

277. Albeverio, Sergio; Koroliuk, Volodymyr; Samoilenko, Igor: Asymptotic Expansion of Semi-Markov Random Evolutions

278. Frehse, Jens; Kassmann, Moritz: Nonlinear Partial Differential Equations of Fourth Order under Mixed Boundary Conditions

279. Juillet, Nicolas: Geometric Inequalities and Generalized Ricci Bounds in the Heisenberg Group

280. DeSimone, Antonio; Grunewald, Natalie; Otto, Felix: A New Model for Contact Angle Hysteresis

281. Griebel, Michael; Oeltz, Daniel: A Sparse Grid Space-Time Discretization Scheme for Parabolic Problems

282. Fattler, Torben; Grothaus, Martin: Strong Feller Properties for Distorted Brownian Motion with Reflecting Boundary Condition and an Application to Continuous N-Particle Systems with Singular Interactions

283. Giacomelli, Lorenzo; Knüpfer, Hans: Flat-Data Solutions to the Thin-Film Equation Do Not Rupture

284. Barbu, Viorel; Marinelli, Carlo: Variational Inequalities in Hilbert Spaces with Measures and Optimal Stopping

285. Philipowski, Robert: Microscopic Derivation of the Three-Dimensional Navier-Stokes Equation from a Stochastic Interacting Particle System

286. Dahmen, Wolfgang; Kunoth, Angela; Vorloeper, Jürgen: Convergence of Adaptive Wavelet Methods for Goal-Oriented Error Estimation; erscheint in: ENUMATH 2005 Proceedings

287. Maes, Jan; Kunoth, Angela; Bultheel, Adhemar: BPX-Type Preconditioners for 2nd and 4th Order Elliptic Problems on the Sphere; erscheint in: SIAM J. Numer. Anal.

288. Albeverio, Sergio; Mazzucchi, Sonia: Theory and Applications of Infinite Dimensional Oscillatory Integrals

289. Holtz, Markus; Kunoth, Angela: B-Spline Based Monotone Multigrid Methods, with an Application to the Pricing of American Options

290. Albeverio, Sergio; Ayupov, Shavkat A.; Kudaybergenov, Karim K.: Non Commutative Arens Algebras and their Derivations

291. Albeverio, Sergio; De Santis, Emilio: Reconstructing Transition Probabilities of a Markov Chain from Partial Observation in Space

292. Albeverio, Sergio; Hryniv, Rostyslav; Mykytyuk, Yaroslav: Inverse Spectral Problems for Bessel Operators

293. Albeverio, Sergio; Hryniv, Rostyslav; Mykytyuk, Yaroslav: Reconstruction of Radial Dirac Operators

294. Abels, Helmut; Kassmann, Moritz: The Cauchy Problem and the Martingale Problem for Integro-Differential Operators with Non-Smooth Kernels

295. Albeverio, Sergio; Daletskii, Alexei; Kalyuzhnyi, Alexander: Random Witten Laplacians: Traces of Semigroups, L^2-Betti Numbers and Index

296. Barlow, Martin T.; Bass, Richard F.; Chen, Zhen-Qing; Kassmann, Moritz: Non-Local Dirichlet Forms and Symmetric Jump Processes

297. Kassmann, Moritz: Harnack Inequalities. An Introduction; erscheint in: Boundary Value Problems

298. Berkels, Benjamin; Burger, Martin; Droske, Marc; Nemitz, Oliver; Rumpf, Martin: Cartoon Extraction based on Anisotropic Image Classification; erscheint in: Vision, Modeling, and Visualization Proceedings

299. Conti, Sergio; Lenz, Martin; Rumpf, Martin: Modeling and Simulation of Magnetic Shape-Memory Polymer Composites

300. Nemitz, Oliver; Rumpf, Martin; Tasdizen, Tolga; Whitaker, Ross: Anisotropic Curvature Motion for Structure Enhancing Smoothing of 3D MR Angiography Data; erscheint in: Journal of Mathematical Imaging and Vision

301. Albeverio, Sergio; Ayupov, Shavkat; Kudaybergenov, Karimbergen: Derivations on the Algebra of Measurable Operators Affiliated with a Type I von Neumann Algebra

302. Buch, Thomas: Embedding and Boundary Analysis for Anisotropic Besov-Morrey Spaces

303. Berkels, Benjamin; Rätz, Andreas; Rumpf, Martin; Voigt, Axel: Identification of Grain Boundary Contours at Atomic Scale

304. Harbrecht, Helmut; Schneider, Reinhold; Schwab, Christoph: Sparse Second Moment Analysis for Elliptic Problems in Stochastic Domains

305. Harbrecht, Helmut: Analytical and Numerical Methods in Shape Optimization